Research article

# N-alkylation of amines for the synthesis of potential antiviral agents: A structural modification approach

Nadia Arrousse [a,b,**], Elyor Berdimurodov [c,d,e,k,*], Mariia Bogacheva [f], Fathiah Zakham [g,h,***], Soukaina Esslali [i], Sghir EL Kadiri [j,****], Mustapha Taleb [b], Olli Vapalahti [g,h]

[a] School of Science and Engineering, Al Akhawayn University in Ifrane, Hassan II avenue, 53000 Ifrane, Morocco
[b] Laboratory of Engineering, Electrochemistry, Modelling and Environment (LIEME), Faculty of Sciences, University Sidi Mohamed Ben Abdellah, Fez, Morocco
[c] Faculty of Chemistry, National University of Uzbekistan, Tashkent, 100034, Uzbekistan
[d] Physics and Chemistry, Western Caspian University, AZ-1001, Baku, Azerbaijan
[e] University of Tashkent for Applied Sciences, Str. Gavhar 1, 100149, Tashkent, Uzbekistan
[f] Viral Zone Research Unit, Faculty of Medicine, University of Helsinki, Finland
[g] Department of Veterinary Biosciences, Faculty of Veterinary Medicine, University of Helsinki, Helsinki, Finland
[h] Faculty of Pharmacy, University of Helsinki, 00014 Helsinki, Finland
[i] Laboratory of Chemistry-Biology Applied to the Environment, Chemistry Department, Faculty of Sciences, Moulay-Ismail University, B.P. 11201, Zitoune, Meknes, Morocco
[j] Laboratory of Applied Chemistry & Environment (LCAE), Faculty of Science, Mohammed First University, Oujda, Morocco
[k] Physics and Chemistry, Tashkent Institute of Irrigation and Agricultural Mechanization Engineers" National Research University, 100000, Tashkent, Uzbekistan

## ARTICLE INFO

## ABSTRACT

The threat of emerging viral outbreaks has increased the need for fast and effective development of therapeutics against emerging pathogens. One approach is to modify the structure of existing therapeutic agents to achieve the desired antiviral properties. Here, we attempted to synthesize a new antiviral compound by modifying the structure of chloroquine using the *N-alkylation* of the primary amine (N1,N1-diethylpentane-1,4-diamine) that is used in chloroquine synthesis. Chloroquine is commonly used to treat malaria. Like chloroquine, chloroquine is used for treating conditions such as rheumatoid arthritis, lupus, and malaria. For instance, in malaria treatment, it targets and inhibits the growth of the malaria parasite, aiding in its elimination from the body. The synthesized compounds MP1, C1, and TT1 were further tested in vitro against the B.1 lineage of SARS-CoV-2. One of the compounds, MP1, demonstrated minor effectiveness, with an IC50 of XX at only a high concentration (at a concentration of 60 μM) and decreased both the number of SARS-CoV-2 copies and the amount of infectious virus. Although the synthesized compounds failed to markedly inhibit SARS-CoV-2, this could be a pontial mechanism for manipulating the drug structure against other pathogens. MP1, TT1, C1, and chloroquine diphosphate were used as ligands for molecular docking to determine the principal interactions between these compounds

* Corresponding author. Faculty of Chemistry, National University of Uzbekistan, Tashkent, 100034, Uzbekistan.
** Corresponding author. School of Science and Engineering, Al Akhawayn University in Ifrane, Hassan II avenue, 53000 Ifrane, Morocco
*** Corresponding author. Department of Veterinary Biosciences, Faculty of Veterinary Medicine, University of Helsinki, Helsinki, Finland.
**** Corresponding author.
*E-mail addresses:* elyor170690@gmail.com (E. Berdimurodov), fathiah.zakham@helsinki.fi (F. Zakham), s.elkadiri@ump.ac.ma (S. EL Kadiri).

and the active site of the protein downloaded from the Protein Data Bank (PDB ID: 6lzg). Finally, ADMET assays were performed on the synthesized compounds to determine their pharmacokinetics and bioavailability.

## 1. Introduction

The N-alkylation of primary amines is a pivotal process in organic synthesis, yielding chemicals widely used in materials chemistry, agro-chemistry, and medicine. This method involves introducing alkyl groups to the nitrogen atom of an amine, significantly altering its solubility, stability, and biological activity. Achieving selective monoalkylation is critical, as excessive alkylation can produce derivatives with reduced or undesirable properties. Traditional techniques typically use alkyl halides or sulfonates combined with bases, while modern methods favour more environmentally friendly substances like alcohols, aldehydes, or carbon dioxide, enhancing sustainability and selectivity [1–4]. Catalysis is importance in improving the efficiency and control of reactions, particularly when using metals such as palladium, nickel, and copper or organocatalysts, which allow for milder reaction conditions. The main difficulties in *N-alkylation* mainly involve attaining a high level of selectivity for monoalkylation and establishing environmentally friendly chemical methods. Constant efforts are being made to decrease the environmental footprint by minimizing waste and utilizing renewable resources and nontoxic solvents. The progress made in medicines is especially noteworthy, as altering the architecture of drugs might result in enhanced pharmacokinetic qualities or decreased toxicity. Similarly, *N-alkylation* plays a crucial role in the fields of agrochemicals and materials science by facilitating the development of highly efficient insecticides and innovative polymers with customized features [5–8]. This underscores its significance in both practical applications and fundamental research.

The increasing prevalence of viral diseases like SARS-CoV-2, the cause of COVID-19, underscores the urgent need for rapid and effective therapeutic drug development. Traditionally, the process of discovering new drugs is time-consuming and resource intensive. However, modifying the chemical structure of existing drugs to enhance their antiviral properties offers significant potential [9–11]. This approach leverages known pharmacodynamics and pharmacokinetics to expedite development and approval processes. Chloroquine, long used to treat malaria and certain autoimmune diseases, is a promising candidate for such modifications due to its structural versatility and established biological interactions. While chloroquine's effectiveness against SARS-CoV-2 remains controversial and not widely accepted for COVID-19 treatment, its structural framework provides a useful foundation for developing new drugs [12–15].

This study focuses on the N-alkylation of a primary amine, specifically N1N1-diethylpentane-14-diamine, commonly used in chloroquine production, to create novel antiviral compounds. This synthetic approach is advantageous as it typically yields high quantities and can significantly alter the biological activity of the original drug. Our aim is to improve antiviral treatment effectiveness by targeting specific structural features while reducing the side effects commonly associated with chloroquine. The subsequent sections detail the synthesis, characterization, and in vitro evaluation of three novel compounds. These compounds were tested for their interactions with viral proteins and assessed for their potential as antiviral drugs against SARS-CoV-2. We conducted molecular docking experiments and ADMET profiling to evaluate the potential of these N-alkylated compounds for further development. Additionally, we targeted SARS-CoV-2 in TMPRSS2-expressing Vero cells to determine the impact of these structural modifications on antiviral efficacy.

## 2. Materials and methods

### 2.1. Synthesis protocols

a General Procedures for Preparing Compounds
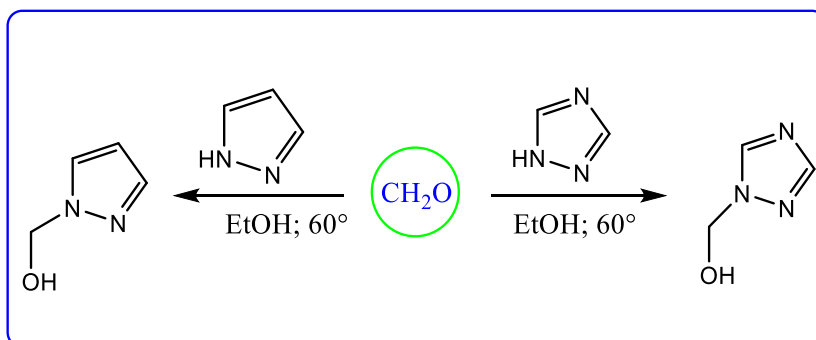


**Scheme 1.** Production of precursor compounds.

The new chemicals were synthesized by the condensation of monoalkylation and dialkylation of (1H-pyrazol-1-yl) methanol and (1H-1,2,4-triazol-1-yl) methanol [16], respectively, (Scheme 1), and the commercial reagent (2-chloro-5-(chloromethyl) pyridine) 97 % (Sigma–Aldrich, CAS number: 70258-18-3) with N1,N1-diethylpentane-1,4-diamine was used to synthesize MP1, TT1, and C1 (Scheme 2).

The synthetic scheme in Fig. 2 illustrates the stepwise process used to synthesize the target compounds MP1, TT1, and C1 from the starting material N1N1-diethylpentane-14-diamine.

*Synthesis of MP1*: MP1 was synthesized by reacting N1N1-diethylpentane-14-diamine with (1H-pyrazol-1-yl) methanol in acetonitrile. The reaction was carried out at room temperature over 3 days. The product was then isolated by liquid-liquid extraction, yielding MP1.

*Synthesis of TT1*: TT1 was produced by condensing N1N1-diethylpentane-14-diamine with two equivalents of (1H-124-triazol-1-yl) methanol in acetonitrile. This reaction occurred at 60 °C with continuous stirring for 6 h, after which TT1 was isolated using a liquid-liquid extraction process.

*Synthesis of C1*: C1 was synthesized by reacting N1N1-diethylpentane-14-diamine with 2-chloro-5-(chloromethyl)pyridine in acetonitrile at room temperature for 1 week. The final product was isolated through liquid-liquid extraction.

Each of these reactions follows standard organic synthesis protocols for alkylation, and the products were characterized using NMR and mass spectrometry to confirm their structures.

## 2.2. Cell viability assay

The VeroE6-TMPRSS2 cell line was provided by Dr. Hepojoki and obtained from a previous study [17]. This cell line is engineered and stored in-house, as outlined in that reference, and does not have an RRID in the ExPASy Cellosaurus database. The VeroE6-TMPRSS2 cell line was authenticated as part of the original engineering and validation process described in Ref. [17]. As the cell line was engineered in-house, no further external authentication was performed beyond routine monitoring. All cell lines in our laboratory cell bank, including the VeroE6-TMPRSS2 line, are routinely tested for mycoplasma contamination using a PCR-based
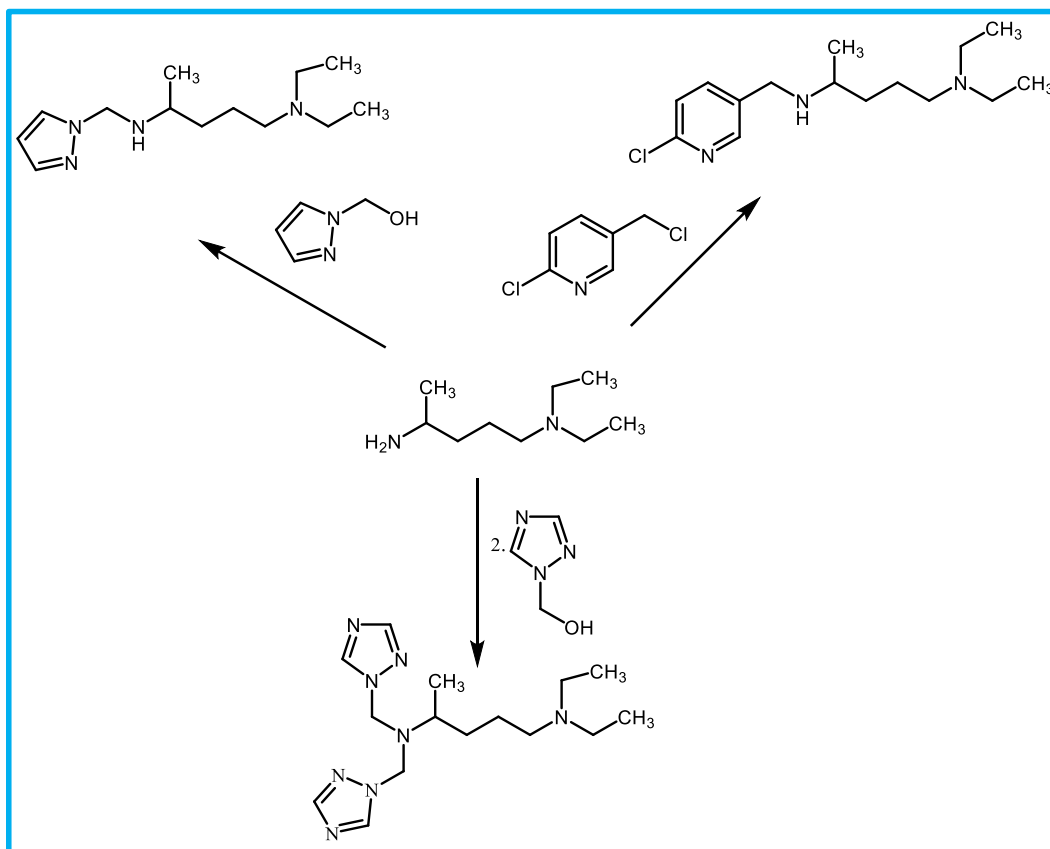


**Scheme 2.** MP1 was synthesized by reacting (1H-pyrazol-1-yl) methanol at room temperature for 3 days. TT1 was prepared by reacting (1H-1,2,4-triazol-1-yl) methanol with N1,N1-diethylpentane-1,4-diamine in acetonitrile at 60 °C for 6 h. C1 was synthesized by condensing 2-chloro-5-(chloromethyl)pyridine with an amine in acetonitrile at room temperature for 1 week. All compounds were isolated by liquid-liquid extraction with $H_2O/CH_2Cl_{anti}$.

assay, ensuring they remain free of contamination. VeroE6-TMPRSS2 cell line were maintained in Minimum Essential Medium (MEM, from Sigma, Catalogue M2279) enriched with 10 % Fetal Bovine Serum (FBS, supplied by Gibco, Catalogue 10270-106), L-glutamine (from Sigma, Catalogue G7513), and a combination of penicillin and streptomycin (also from Sigma, Catalogue P0781). When setting up infections, the MEM was adjusted to contain only 2 % FBS but still included L-glutamine, penicillin, and streptomycin. These cells were plated at a density of 30,000 cells per well in 96-well plates with white sides (from PerkinElmer, Catalogue 6005070). The chemical compounds initially synthesized were formulated as 1 mM stock solutions in 0.1 % DMSO. Prior to the experiments, these solutions were further diluted to final concentrations ranging from 100 μM down to 0.78125 μM for virus infection assays. The cells were exposed to these varying concentrations and incubated at 37 °C with 5 % $CO_2$ for an hour. The negative control involved the treatment of cells with only 0.1 % DMSO. The infection was performed by employing the SARS-CoV-2 B.1 lineage, isolated as described by Cantuti-Castelvetri et al., 2020 [18], with a multiplicity of infection (MOI) of 0.5. Non-infected cells, termed MOCK, served as a positive control to gauge the effectiveness of the viral inhibition. Following a 48 or 60-h incubation, the system was replaced, and CellTiter-Glo 2.0 reagent (Promega, Catalogue G9243) was added for 15 min at room temperature to assess cell viability. The luminescence emitted, which correlates directly with the quantity of cellular ATP, was measured using a HIDEX Sense microplate reader. The viability of MOCK-infected cells was set at 100 %, and the antiviral efficacy of the test compounds was evaluated based on their capacity to enhance cell viability relative to the untreated virus-infected cells.

## 2.3. Assessment of the antiviral effectiveness of synthesized compounds via changes in viral infection

The VeroE6-TMPRSS2-H10 cells were distributed in 48-well plates with a density of 40,000 cells per well. Following a 24-h period, the cells were exposed to SARS-CoV-2 lineage B.1 at a multiplicity of infection (MOI) of 0.25 and kept in an incubator at a temperature of 37 °C and a carbon dioxide concentration of 5 % for 1 h. Subsequently, the system including the virus was extracted, and the cells were washed twice with 1x PBS. The selected compounds at the concentrations chosen after the cell viability assay were added to the cells in three replicates. DMSO (0.1 %) in the medium for infection was used as a control. One hour post infection (hpi), a cell supernatant sample was collected for RT–PCR. After 48 h of incubation at 37 °C and 5 % $CO_2$, the second cell supernatant medium sample (48 hpi) for RT–PCR and samples for the TCID50 test were collected. Viral RNA Mini Kit (Qiagen, 52906) was performed to extract Viral RNA. The quantification of SARS-CoV-2 copy number was accomplished by qRT-PCR utilizing primers, probes, and an in vitro generated control for RNA-dependent RNA polymerase (RdRp) as outlined in the studies conducted by Corman et al., 2020 and Lin et al., 2021 [19,20]. The quantification of viral concentrations was conducted using a TCID50 test on VeroE6 (ATCC® CRL-1586) cells. Forty-eight hpi samples collected from each well of a 48-well plate were sequentially diluted 10-fold in medium for viral infection and added to VeroE6 cells in four replicates. The cells were cultured for 5 days at a temperature of 37 °C and a carbon dioxide concentration of 5 %. After that, they were treated with a 10 % formaldehyde solution for 30 min at room temperature and then stained with crystal violet. The infectious virus titres after treatment with the test compounds were compared with those of the control virus without the test compounds.

## 2.4. Statistical analysis of in vitro data

The statistical significance of changes between conditions was analysed using GraphPad Prism 9.2.0 software. The variable "N" denotes the quantity of wells utilized under the specified circumstances. Dunnett's multiple comparison investigation (one-way analysis of variance (ANOVA)) was done to determine the statistical significance. If the distribution of the sample population deviated from normality, Dunn's multiple comparisons tests were done with either the Kruskal–Wallis exam or Mann–Whitney exam. Significance was attributed to differences with adjusted p-values of less than 0.05 (*), less than 0.01 (**), less than 0.001 (***), and less than 0.0001 (****).

## 2.5. In silico pharmacokinetics ADMET study

To examine the pharmacokinetic profile of the synthesized compounds (C1-MP1 and TT1), an in silico study [34–38] was done by calculating the ADMET (Toxicity, Excretion, Metabolism, Distribution and Adsorption) performances [21] using the pkCSM online server (http://biosig.unimelb.edu.au/pkcsm/) [22].

## 2.6. Molecular docking analysis

In order to comprehend the primary structural prerequisites [23] to ascertain the fundamental interactions between the protein (PDB: ID 6lzg) and the different produced chemicals, a molecular docking investigation was conducted [24]. We obtained the crystallographic structure of the protein (PDB code: 6lzg) from the Protein Data Bank (https://www.rcsb.org/) [25]. The protein was created by introducing polar hydrogen atoms, while the removal of water molecules was achieved utilizing Discovery Studio software. The AutoDock 1.5.6 software was employed to process of molecular docking [26].

## 3. Results and discussion

### 3.1. Characterization of the synthesis of compounds

$N^4$-[(6-Chloropyridin-3-yl)methyl] -$N_1$,$N_1$-diethylpentane-1,4-diamine (C1) (oil): Boiling point = 91–92 °C, Yield = 74 %, $^1$H NMR (400 MHz, CDCl$_3$): δ 0.98 (t, $J$ = 7.1 Hz, 6H, 1.01 (d, $J$ = 6.3 Hz, 3H), 1.46–1.32 (m, 4H), 2.38–2.23 (m, 2H), 2.46–2.39 (m, 1H), 2.47 (q, $J$ = 7.2 Hz, 4H), 2.59 (td, $J$ = 6.4, 5.3 Hz, 1H), 3.78, 3.70 (2d, $J$ = 13.7 Hz, 2H), 7.19 (d, $J$ = 8.2 Hz, 1H)), 7.60 (dd, $J$ = 8.2, 2.5 Hz, 1H), 8.24 (dd, $J$ = 2.5, 0.7 Hz, 1H). $^{13}$C NMR (CDCl$_3$): δ 158.33, 149.49, 138.78, 123.93, 52.92, 52.88, 52.45, 47.56, 46.75, 38.05,
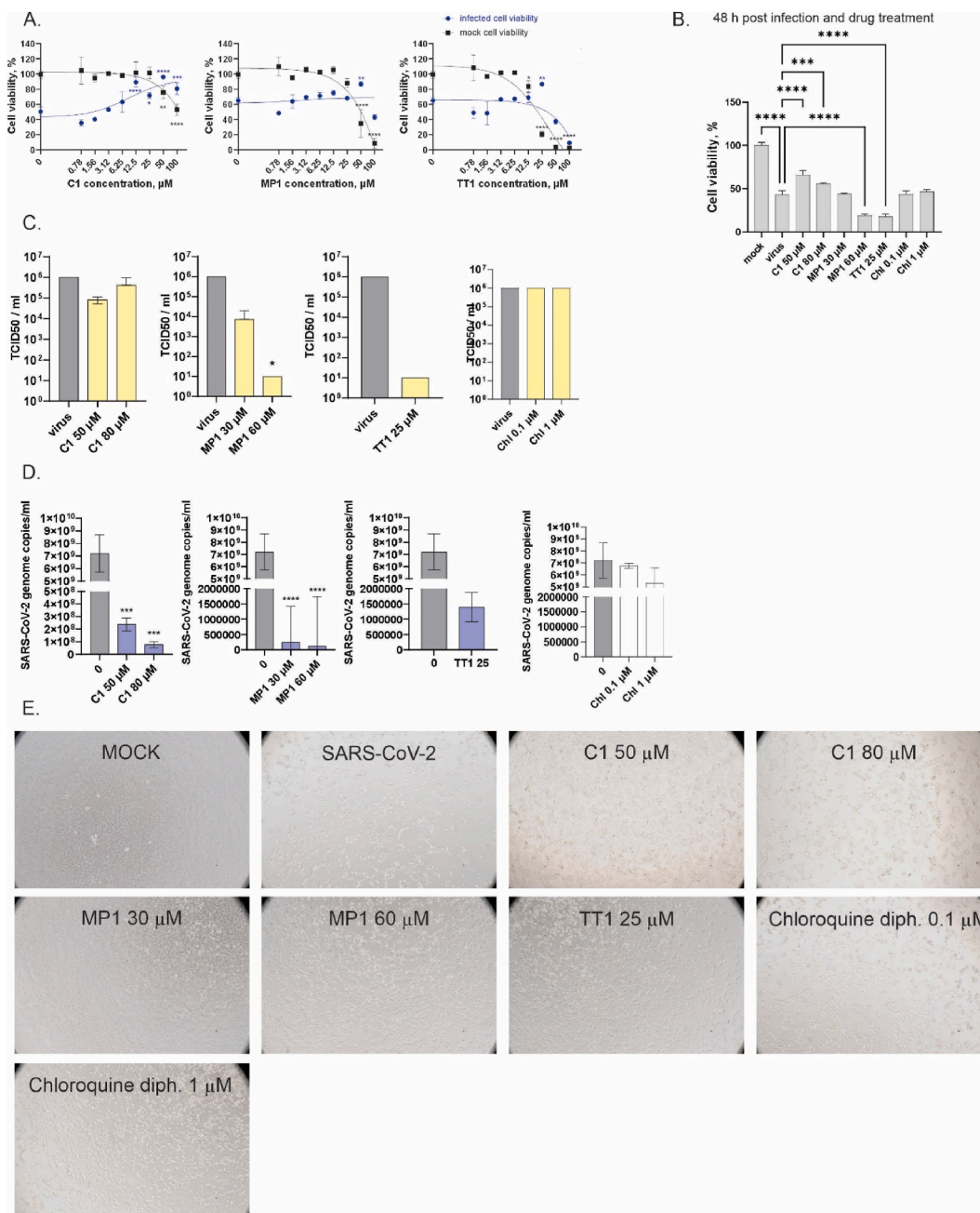


**Fig. 1.** The in vitro study assessed the impact of chloroquine derivatives on VeroE6-TMPRSS2-H10 cells and SARS-CoV-2 (B.1). C1 and MP1 showed increased infected cell viability at high concentrations but were toxic to uninfected cells, with IC50 values of 8.606 and 1.377, respectively; TT1's IC50 was undetected. Cell viability, viral particle production, SARS-CoV-2 copy numbers, and cell morphology were evaluated after treatment with C1, MP1, TT1, and chloroquine diphosphate.

34.82, 23.87, 23.42, 11.99. MS (EI) M+. = 284.

**N$^4$, N$^4$-bis((1H-1,2,4-triazol-1-yl)methyl)-N$_1$,N$_1$-diethylpentane-1,4-diamine (TT1)** (oil): Boiling point = 94–95 °C, yield = 81 %; $^1$H NMR (400 MHz, CDCl$_3$): δ 0.50 (d, $J$ = 6.7 Hz, 6H), 0.58 (t, $J$ = 7.2 Hz, 6H), 1.12–0.81 (m, 4H), 1.98–1.83 (m, 2H), 2.07 (q, $J$ = 7.2 Hz, 4H), 2.72 (h, $J$ = 7 Hz, 1H), 4.87, 4.93 (2d, $J$ = 14.3 Hz, 2H), 7.95 (s, 1H), 7.56 (s, 1H). $^{13}$C NMR (400 MHz, CDCl$_3$) δ 151.62, 146.55, 143.00, 71.75, 63.86, 56.11, 52.1, 46.36, 32.67, 23.74, 17.89, 11.24. MS (EI) M+. = 320.

**N$^4$-((1H-pyrazol-1-yl)methyl)-N$_1$,N$_1$-diethylpentane-1,4-diamine (MP1)** (oil): Boiling point = 87–88 °C, yield = 72 %, $^1$H NMR (400 MHz, CDCl$_3$): 0.87 (t, $J$ = 7.2 Hz, 6H), 0.95 (d, $J$ = 6.3 Hz, 1H), 1.43–1.08 (m, 4H), 2.26–2.17 (m, 2H), 2.32–2.26 (m, 1H), 2.39 (q, $J$ = 7.2 Hz, 4H), 2.78 (h, $J$ = 6.3 Hz, 1H), 4.9, 4.86 (2d, $J$ = 13.5 Hz, 2H), 6.13 (t, $J$ = 2.0 Hz, 1H), 7.36 (d, $J$ = 2.3 Hz, 1H), 7.42 (d, $J$ = 2.3 Hz, 1H). $^{13}$C NMR (400 MHz, CDCl$_3$): δ 139.50, 128.70, 105.12, 63.33, 52.92, 48.66, 46.65, 34.65, 23.88, 19.87, 11.53. MS (EI) M+. = 238.

The synthesized compounds—C1, TT1, and MP1—were characterized using boiling point determination, $^1$H and $^{13}$C NMR spectroscopy, and mass spectrometry (MS).

*N4-[(6-Chloropyridin-3-yl)methyl]-N1,N1-diethylpentane-1,4-diamine (C1)*: the boiling point of 94–95 °C is slightly higher than C1, suggesting similar stability. The signals at δ 0.98 (t, $J$ = 7.1 Hz, 6H) correspond to the terminal methyl protons of the ethyl groups. The multiplet at δ 1.46–1.32 is assigned to the methylene protons, and the signals between δ 2.38–2.59 represent the protons near the nitrogen atom. The aromatic protons appear in the region of δ 7.19–8.24, confirming the presence of a chloropyridine ring. The signals
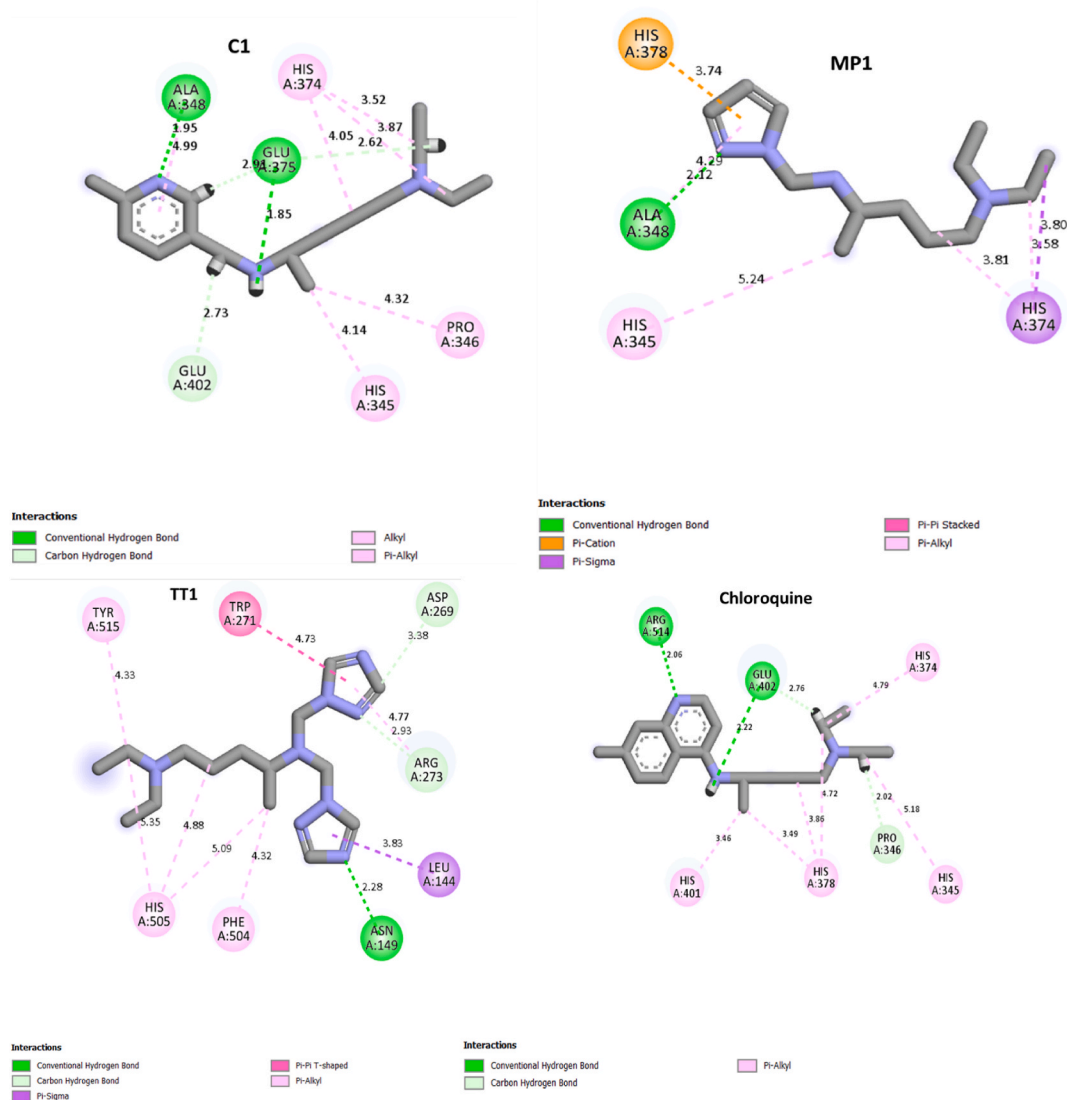


**Fig. 2.** Docking results of synthesized compounds and chloroquine with the active site in the protein (PDB ID: 6lzg); the binding energies corresponding to C1 (−7.64 kcal), TT1 (−4.47 kcal), MP1 (−3.67 kcal) and chloroquine (−6.15 kcal). All the compounds present hydrogen bonds; the synthesized C1 and chloroquine have two hydrogen bonds, while the other molecules, MP1 and TT1, present one hydrogen bond.

at δ 158.33, 149.49, and 138.78 correspond to the carbons in the chloropyridine ring, while the signals between δ 52.92–11.99 represent the alkyl chain and ethyl groups. The molecular ion peak at *m/z* 284 confirms the molecular weight of the compound, matching the expected value.

*N4,N4-bis((1H-1,2,4-triazol-1-yl)methyl)-N1,N1-diethylpentane-1,4-diamine (TT1)*: The boiling point of 94–95 °C is slightly higher than C1, suggesting similar stability. The signal at δ 0.50 (d, J = 6.7 Hz, 6H) corresponds to the methyl groups, while δ 0.58 (t, J = 7.2 Hz, 6H) indicates the terminal ethyl groups. The peaks at δ 4.87 and 4.93 (2d, J = 14.3 Hz) correspond to the triazole methyl groups, while the signals at δ 7.95 and 7.56 confirm the presence of the triazole ring protons. The signals at δ 151.62, 146.55, and 143.00 correspond to the carbons of the triazole rings, and the peaks at δ 71.75–11.24 represent the alkyl chain. The molecular ion peak at *m/z* 320 confirms the molecular weight of TT1, consistent with its expected structure.

*N4-((1H-pyrazol-1-yl)methyl)-N1,N1-diethylpentane-1,4-diamine (MP1)*: MP1 shows a slightly lower boiling point (87–88 °C), indicative of its relatively lower molecular weight compared to C1 and TT1. The signal at δ 0.87 (t, J = 7.2 Hz, 6H) is attributed to the ethyl group protons. The multiplets between δ 1.43–2.78 correspond to the methylene protons, and the peaks at δ 6.13–7.42 represent the pyrazole ring protons, confirming the incorporation of the pyrazole moiety. The signals at δ 139.50, 128.70, and 105.12 are attributed to the carbons of the pyrazole ring, while δ 63.33–11.53 represent the alkyl chain and ethyl groups. The molecular ion peak at *m/z* 238 confirms the molecular weight of MP1, aligning with the expected structure.

### 3.2. In vitro tests of synthesized compounds

Fig. 1 illustrates the in vitro effects of the synthesized compounds (C1, MP1, TT1) on SARS-CoV-2 infection and cell viability in VeroE6-TMPRSS2-H10 cells. The data show that C1 and MP1 significantly improved infected cell viability at higher concentrations, while TT1's effect was less pronounced. However, these compounds also exhibited toxicity to uninfected cells, especially C1 and MP1 at their highest concentrations. MP1 demonstrated a reduction in the number of infectious virus particles, while both C1 and MP1 decreased viral genome copy numbers at tested concentrations. TT1 had no significant effect on viral particle production or genome copy reduction. This figure highlights the antiviral potential and cytotoxicity profiles of the synthesized compounds.

An in vitro study of chloroquinoline derivative compounds included two testing protocols. Initially, we tested the ability of 8 concentrations of each compound to prevent virus-induced cytopathic effects (CPEs). After 1 h of treatment with the synthesized compounds, some of the cells were infected with SARS-CoV-2 WT at an MOI of 0.5 infectious units (i.u.) per cell for 48 h (n = 2). Another part served as a drug cytotoxicity measurement (n = 3). All the compounds significantly rose the possibility of infected cells at the tested concentrations (Fig. 1A). We selected the lowest concentrations of the selected chemicals that escalated cell possibility (50 and 80 μM C1, 30 and 60 μM MP1, and 25 μM TT1) to determine how they affect virus production. Chloroquine diphosphate at concentrations of 0.1 and 1 μM was used as a negative control. The cells were first infected with SARS-CoV-2 at an MOI of 0.5 for 1 h, after which the virus was removed, and the cells were treated with the abovementioned concentrations of the compounds. At 48 hpi, the viability of infected cells treated with 60 μM MP1 or 25 μM TT1 was significantly lower than that of infected and untreated cells (Fig. 1B). The amount of infectious virus particles decreased only after treatment of cells with 60 μM MP1 (Fig. 1C), while the number of viral genome copies decreased after treatment with C1 and MP1 at both tested concentrations (Fig. 1D). All the compounds except for MP1 at 30 μM disturbed the cell morphology or noticeably altered the cell number (Fig. 1E).

### 3.3. In silico pharmacokinetics ADMET study

It was performed an in silico ADMET study on the synthesized compounds and chloroquine using pkCSM, and the obtained details were indicated in Table 1. A low absorbance in the human intestine is considered an absorbance value < 30 %. C1, MP1, and TT1 all had absorbance values > 85 %, suggesting that these synthesized compounds have good absorbance. The significant values for the steady-state volume of distribution (VDss, log L/kg) are >0.45 [27]. The VDss of C1, MP1, and TT1 were 1.248, 1.049, and 0.682, respectively, indicating a high volume of distribution. In order to examine how these molecules interact with various membrane barriers in the body, we made predictions about the values of the blood-brain barrier (BBB) and central nervous system (CNS) transporters. A value > 0.3 is considered good BBB permeability, and a value <−1 is considered poor [28]. Compound C1 has good BBB permeability (0.477). Compound C1 was found to be the substrate and the inhibitor of CYP2D6. Clearance is a parameter that describes the relationship between the concentration of a drug in the body and the rate at which it is eliminated. Consequently, all new compounds have acceptable effects on drug persistence in the body. Unlike chloroquine, not all the compounds synthesized have AMES toxicity. The in silico results suggested that C1, MP1, and TT1 may be drug candidates.

Overall, the synthesized chloroquine derivatives C1, MP1, and TT1 exhibit promising antiviral activity against SARS-CoV-2 with varying degrees of efficacy. C1 and MP1 showed enhanced infected cell viability at high concentrations, though with toxicity to uninfected cells, while TT1's IC50 was not detectable. In silico ADMET studies indicate that these compounds have high absorbance, substantial volume of distribution, and, notably, C1 has favourable blood-brain barrier permeability and interacts with CYP2D6. Additionally, the synthesized compounds do not exhibit AMES toxicity, suggesting a safer profile compared to chloroquine. These results collectively suggest that C1, MP1, and TT1 are viable candidates for further development and evaluation as potential therapeutic agents for COVID-19.

### 3.4. Molecular docking tests

A docking study was utilized to ascertain the primary interactions between the produced chemicals, chloroquine, and the protein's

**Table 1**
In silico ADMET prediction of C1, MP1, TT1, and chloroquine.

| N | Adsorption | Distribution | | | Metabolism | | | | | | | Excretion | Toxicity |
|---|---|---|---|---|---|---|---|---|---|---|---|---|---|
| | | | | | Substrate | | Inhibitor | | | | | | |
| | Intestinal Absorption (Human) | VDss (Human) | BBB Permeability | CNS Permeability | CYP | | | | | | | Total Clearance | Ames Toxicity |
| | | | | | 2D6 | 3A4 | 1A2 | 2C19 | 2C9 | 2D6 | 3A4 | | |
| | Numeric (% absorbed) | Numeric (log Lkg-) | Numeric (log BB) | Numeric (log PS) | Categorical (yes/no) | | | | | | | Numeric (log mL min$^{-1}$ kg$^{-1}$) | Categorial (Yes/No) |
| chloro | 89.95 | 1.332 | 0.349 | −2.191 | Yes | Yes | No | No | No | Yes | No | 1.092 | Yes |
| C1 | 91.936 | 1.248 | 0.477 | −3.134 | Yes | No | No | No | No | Yes | No | 1.135 | No |
| MP1 | 93.35 | 1.049 | 0.138 | −3.366 | No | No | No | No | No | No | No | 1.205 | No |
| TT1 | 85.175 | 0.628 | −1.133 | −3.302 | No | Yes | No | No | No | No | No | 0.844 | No |

active site. This research also aimed to assess the affinity of the ligand-receptor combination (Fig. 2).

For C1 and chloroquine, the presence of two hydrogen-type interactions between Ala-348 (1.95 Å), Glu-375 (1.85 Å), Arg-514 (2.06 Å), and Glu-402 (2.22 Å) was observed. TT1 and MP1 showed a single hydrogen-type interaction with Asn-149 (2.28 Å) and Ala-348 (2.12 Å), respectively. Compared to chloroquine, the synthesized molecule (C1) has the lowest binding energy (−7.64 kcal).

Since the emergence of COVID-19, the effectiveness of hydroxychloroquine and chloroquine has been debated. Chloroquine is a safe, inexpensive, and effective antimalarial treatment that has been used for 70 years. Chloroquine was employed against autoimmune diseases and viral infections, such as Zika virus, dengue virus, and other coronavirus diseases [29]. In the first step of COVID-19 pandemic research, many research conducted using computer simulations, laboratory experiments, animal testing, and clinical trials provided evidence in favour of using chloroquine and its derivatives as a potential treatment for COVID-19 [6–9]. Recently, super-resolution imaging of mammalian cell cultures showed that hydroxychloroquine affects the clustering of the ACE2 receptor with both endocytic lipids and phosphatidylinositol 4,5 bisphosphate clusters prior to inhibiting cathepsin-L, depending on tissue cholesterol levels [30].

Moreover, the toxicity of chloroquine and hydroxychloroquine poses a serious risk for their use at higher concentrations, primarily due to cardiovascular side effects as well as phospholipidosis [31]. Therefore, we attempted to use an *N-alkylation* approach to study potentially more effective and less toxic alternatives. Of the studied compounds, only MP1 decreased the SARS-CoV-2 copy number at both tested concentrations and decreased the amount of infectious virus, and the effective concentrations were too high to support further studies on its use against SARS-CoV-2.

## 4. Conclusion

In this study, we synthesized three novel compounds, MP1, C1, and TT1, using N1N1-diethylpentane-14-diamine as the principal reactive agent. These compounds were designed as potential antiviral agents against SARS-CoV-2, inspired by the structure of chloroquine. Despite achieving good yields, the modification approach enhance the antiviral properties of chloroquine. Specifically, the synthesized compounds failed to significantly inhibit SARS-CoV-2 in vitro, suggesting that the selected N-alkylation strategy may be suitable for developing effective antiviral agents against this virus.

However, our findings do highlight the importance of exploring different structural modifications and synthesis pathways in drug development. While MP1 showed minor effectiveness at high concentrations, further optimization and testing of similar compounds could provide valuable insights for future research. Moreover, the molecular docking and ADMET profiling conducted in this study underscore the need for comprehensive evaluations of pharmacokinetic properties and potential toxicity in drug design.

## CRediT authorship contribution statement

**Nadia Arrousse:** Writing – original draft, Formal analysis, Data curation, Conceptualization. **Elyor Berdimurodov:** Writing – review & editing, Project administration, Methodology. **Mariia Bogacheva:** Writing – review & editing, Software, Formal analysis. **Fathiah Zakham:** Writing – review & editing, Project administration, Funding acquisition, Formal analysis. **Soukaina Esslali:** Supervision, Project administration, Methodology. **Mustapha Taleb:** Visualization, Validation, Resources. **Olli Vapalahti:** Project administration, Methodology, Data curation.

## Declaration of competing interest

The authors declare that they have no known competing financial interests or personal relationships that could have appeared to influence the work reported in this paper.

## Acknowledgements

## References

[1] A.J.B. Kreutzberger, et al., SARS-CoV-2 requires acidic pH to infect cells, Proc. Natl. Acad. Sci. USA 119 (38) (2022) e2209514119.
[2] G. Abdolmaleki, et al., A comparison between SARS-CoV-1 and SARS-CoV2: an update on current COVID-19 vaccines, Daru 30 (2) (2022) 379–406.
[3] W. Ni, et al., Role of angiotensin-converting enzyme 2 (ACE2) in COVID-19, Crit. Care 24 (2020) 1–10.
[4] Y. Chen, Q. Liu, D. Guo, Emerging coronaviruses: genome structure, replication, and pathogenesis, J. Med. Virol. 92 (4) (2020) 418–423.
[5] M.J. Vincent, et al., Chloroquine is a potent inhibitor of SARS coronavirus infection and spread, Virol. J. 2 (2005) 1–10.
[6] N. Baildya, N.N. Ghosh, A.P. Chattopadhyay, Inhibitory capacity of Chloroquine against SARS-COV-2 by effective binding with Angiotensin converting enzyme-2 receptor: an insight from molecular docking and MD-simulation studies, J. Mol. Struct. 1230 (2021) 129891.
[7] J. Liu, et al., Hydroxychloroquine, a less toxic derivative of chloroquine, is effective in inhibiting SARS-CoV-2 infection in vitro, Cell discovery 6 (1) (2020) 16.
[8] J. Gao, Z. Tian, X. Yang, Breakthrough: chloroquine phosphate has shown apparent efficacy in treatment of COVID-19 associated pneumonia in clinical studies, Bioscience trends 14 (1) (2020) 72–73.

[9]  P. Gautret, et al., Hydroxychloroquine and azithromycin as a treatment of COVID-19: results of an open-label non-randomized clinical trial, Int. J. Antimicrob. Agents 56 (1) (2020) 105949.

[10] Á. Avezum, et al., Hydroxychloroquine versus placebo in the treatment of non-hospitalised patients with COVID-19 (COPE–Coalition V): a double-blind, multicentre, randomised, controlled trial, The Lancet Regional Health–Americas 11 (2022).

[11] K. Thomson, H. Nachlis, Emergency use authorizations during the COVID-19 pandemic: lessons from hydroxychloroquine for vaccine authorization and approval, JAMA 324 (13) (2020) 1282–1283.

[12] I.S. Schwartz, D.R. Boulware, T.C. Lee, Hydroxychloroquine for COVID19: the curtains close on a comedy of errors, The Lancet Regional Health–Americas 11 (2022).

[13] D.J. Browning, Hydroxychloroquine and Chloroquine Retinopathy, Springer, 2014.

[14] P. Biswas, et al., Candidate antiviral drugs for COVID-19 and their environmental implications: a comprehensive analysis, Environ. Sci. Pollut. Control Ser. 28 (42) (2021) 59570–59593.

[15] B.R.H. Sturrock, T.J.T. Chevassut, Chloroquine and COVID-19–a potential game changer? Clin. Med. 20 (3) (2020) 278–281.

[16] M.S. Pevzner, et al., Heterocyclic nitro compounds. 25. 1-Hydroxymethyl-3-nitro-1, 2, 4-triazoles and their derivatives, Chem. Heterocycl. Compd. 16 (1980) 189–194.

[17] J. Rusanen, et al., A generic, scalable, and rapid time-resolved Förster resonance energy transfer-based assay for antigen detection—SARS-CoV-2 as a proof of concept, mBio 12 (3) (2021) 10–1128.

[18] L. Cantuti-Castelvetri, et al., Neuropilin-1 facilitates SARS-CoV-2 cell entry and infectivity, Science 370 (6518) (2020) 856–860.

[19] J.-w. Lin, et al., Genomic monitoring of SARS-CoV-2 uncovers an Nsp1 deletion variant that modulates type I interferon response, Cell Host Microbe 29 (3) (2021) 489–502.

[20] V.M. Corman, et al., Detection of 2019 novel coronavirus (2019-nCoV) by real-time RT-PCR, Euro Surveill. 25 (3) (2020) 2000045.

[21] M. Rudrapal, et al., Explainable artificial intelligence-assisted virtual screening and bioinformatics approaches for effective bioactivity prediction of phenolic cyclooxygenase-2 (COX-2) inhibitors using PubChem molecular fingerprints, Mol. Divers. (2024) 1–20.

[22] A.R. Issahaku, et al., Characterization of the binding of MRTX1133 as an avenue for the discovery of potential KRASG12D inhibitors for cancer therapy, Sci. Rep. 12 (1) (2022) 17796.

[23] M. Rudrapal, et al., Dual synergistic inhibition of COX and LOX by potential chemicals from Indian daily spices investigated through detailed computational studies, Sci. Rep. 13 (1) (2023) 8656.

[24] A.R. Issahaku, et al., Discovery of potential KRAS-SOS1 inhibitors from South African natural compounds: an in silico approach, ChemistrySelect 8 (24) (2023) e202300277.

[25] J.A. Ezugwu, et al., Design, synthesis, molecular docking, molecular dynamics and in vivo antimalarial activity of new dipeptide-sulfonamides, ChemistrySelect 7 (5) (2022) e202103908.

[26] A. Kouranov, et al., The RCSB PDB information portal for structural genomics, Nucleic Acids Res. 34 (suppl_1) (2006) D302–D305.

[27] N. Moussa, A. Hassan, S. Gharaghani, Pharmacophore model, docking, QSAR, and molecular dynamics simulation studies of substituted cyclic imides and herbal medicines as COX-2 inhibitors, Heliyon 7 (4) (2021) e06605.

[28] K.B. Lokhande, et al., Molecular docking and simulation studies on SARS-CoV-2 Mpro reveals Mitoxantrone, Leucovorin, Birinapant, and Dynasore as potent drugs against COVID-19, J. Biomol. Struct. Dyn. 39 (18) (2021) 7294–7305.

[29] K. Tabti, et al., Molecular modelling of antiproliferative inhibitors based on SMILES descriptors using Monte-Carlo method, docking, MD simulations and ADME/Tox studies, Mol. Simulat. 48 (17) (2022) 1575–1591.

[30] E.-R. Mohammed, et al., QSAR, molecular docking, ADMET properties in silico studies for a series of 7-propanamide benzoxaboroles as potent anti-cancer agents, Chin. J. Anal. Chem. 50 (12) (2022) 100163.

[31] R. Abdizadeh, et al., Investigation of pyrimidine analogues as xanthine oxidase inhibitors to treat of hyperuricemia and gout through combined QSAR techniques, molecular docking and molecular dynamics simulations, J. Taiwan Inst. Chem. Eng. 113 (2020) 72–100.